Princeton Plasma Physics Laboratory

PPPL-4069

PPPL-4069

# Kinetic Damping of Toroidal Alfvén Eigenmodes

G.Y. Fu, H.L. Berk, and A. Pletzer

May 2005

Prepared for the U.S. Department of Energy under Contract DE-AC02-76CH03073.

# PPPL Report Disclaimers

## Full Legal Disclaimer



## Trademark Disclaimer



# PPPL Report Availability

This report is posted on the U.S. Department of Energy's Princeton Plasma Physics Laboratory Publications and Reports web site in Fiscal Year 2005. The home page for PPPL Reports and Publications is: http://www.pppl.gov/pub_report/

## Office of Scientific and Technical Information (OSTI):

Available electronically at: http://www.osti.gov/bridge.

Available for a processing fee to U.S. Department of Energy and its contractors, in paper from:

U.S. Department of Energy
Office of Scientific and Technical Information
P.O. Box 62
Oak Ridge, TN 37831-0062

Telephone: (865) 576-8401

Fax: (865) 576-5728

E-mail: reports@adonis.osti.gov

## National Technical Information Service (NTIS):

This report is available for sale to the general public from:

U.S. Department of Commerce
National Technical Information Service
5285 Port Royal Road
Springfield, VA 22161

Telephone: (800) 553-6847

Fax: (703) 605-6900

Email: orders@ntis.fedworld.gov

Online ordering: http://www.ntis.gov/ordering.htm

# Kinetic Damping of Toroidal Alfvén Eigenmodes

G. Y. Fu[a], H. L. Berk[b], A. Pletzer[c]

[a] *Princeton Plasma Physics Laboratory, Princeton, New Jersey 08543*

[b] *Institute for Fusion Studies, Austin, Texas 78712*

[b] *Geophysical Fluid Dynamics Laboratory, Princeton, New Jersey 08542*

(April 26, 2005)

## Abstract

The damping of Toroidal Alfvén Eigenmodes in JET plasmas is investigated by using a reduced kinetic model. Typically no significant damping is found to occur near the center of the plasma due to mode conversion to kinetic Alfvén waves. In contrast, continuum damping from resonance near the plasma edge may be significant, and when it is, it give rise to damping rates that are compatible with the experimental observations.

## I. INTRODUCTION

A key issue in determining stability criteria of energetic particle-driven Alfvén modes in burning plasma experiments, is to properly describe background damping due to kinetic effects. Since the discovery of a Toroidal Alfvén Eigenmode (TAE) [1], extensive work has been done on its damping mechanisms. In the limit of ideal MHD theory, the TAEs have discrete real frequencies located within the toroidicity-induced continuum gaps. However, when the kinetic effects of thermal electrons and ions are taken into account, the TAEs will damp due to various dissipative processes such as electron Landau damping [2], ion Landau damping [3], collisional damping [4,5] and continuum damping [6]. The damping rates can usually be calculated perturbatively using the MHD mode structure obtained in an ideal MHD code. TAEs are also affected from non-perturbative "radiative" damping due to coupling (or mode conversion) to kinetic Alfvén waves (KAW) [7,8]. Despite substantial work over many years on this topic, a complete understanding of this damping mechanism is still lacking. This is highlighted by a recent comparison of TAE damping models with measured TAE damping rates in JET plasmas [9]. It was found that the measured damping rates of an n=1 TAE mode in JET are much larger than the radiative damping rate as calculated locally by the NOVA-K code [10] (all other damping mechanisms such as electron and ion Landau damping, collisional damping, are also much smaller than the measured damping rates in this case). On the other hand, global gyrokinetic calculations from the PENN code yielded damping rates comparable to experimental values for similar plasmas [11]. The results of the PENN code showed that the main damping is due to mode conversion to kinetic Alfvén wave near the center of plasma. In this work, we have developed a global reduced kinetic model in order to elucidate the key physics and to assess whether mode conversion can occur near the center of plasma when this region is not close to the main continuum gap. We will show that our global kinetic calculations, when the edge density is not particularly low, yield smaller damping rates than is observed experimentally. The low damping rate is consistent with the predictions of a local "radiative" damping model.

However, we observe that with a low edge density, continuum damping due to resonance near the edge is likely to be excited, and this mechanism gives damping rates comparable to what is observed experimentally. We conjecture that it is the wave physics in the edge, which is quite complex and only roughly treated in this work, that is responsible for the damping rates in the JET plasmas.

The paper is organized as follows. Sec. II describes a reduced kinetic model used for our analysis of kinetic damping of TAE's. Sec. III briefly describes the cubic finite element method that is used to obtain the solutions of the fourth-order equations that couple the TAE's to the KAW's. Section IV presents our numerical results of kinetic damping calculations for a model tokamak equilibrium and for an experimental JET plasma where the damping rate of an n=1 TAE was measured. In Sec. V, we discuss the relationship between this work and previous work. Finally, conclusions are given in Sec. VI.

## II. REDUCED KINETIC MODEL

We start from coupled reduced kinetic equations for shear Alfvén waves in toroidal geometry in the limit of large aspect ratio and low beta:

$$\nabla_\perp^2 g_{Km}\frac{1}{\rho}\nabla_\perp\rho\nabla_\perp\Phi_m + L_m\Phi_m = L_{m-1}\Phi_{m-1} + L_{m+1}\Phi_{m+1} \tag{1}$$

$$\begin{aligned}
L_m &= \frac{1}{r}\frac{d}{dr}r(\frac{\omega^2}{V_A^2} - k_{\|m}^2)\frac{d}{dr} - (\frac{\omega^2}{V_A^2} - k_{\|m}^2)\frac{m^2}{r^2} + (k_{\|m}^2)'\frac{1}{r} \\
L_{m-1} &= \frac{1}{r}\frac{d}{dr}r\hat{\epsilon}\frac{\omega^2}{V_A^2}\frac{d}{dr} + 2\frac{\omega^2}{V_A^2}\Delta'\frac{m(m-1)}{r^2} \\
L_{m+1} &= \frac{1}{r}\frac{d}{dr}r\hat{\epsilon}\frac{\omega^2}{V_A^2}\frac{d}{dr} + 2\frac{\omega^2}{V_A^2}\Delta'\frac{m(m+1)}{r^2} \\
g_{Km} &= k_{\|m}^2\left[\frac{3}{8}\rho_i^2 + \frac{1}{2}\rho_s^2\frac{1+i\hat{\nu}Z(\xi)}{1+\xi Z(\xi)}\right]
\end{aligned} \tag{2}$$

where $\Phi_m$ is the electric potential with the subscript $m$ being the poloidal model number. Here the operator $L_m$ corresponds to the ideal MHD equation for shear Alfvén waves in

a cylinder with $m$ being the poloidal mode number, $\omega$ the mode frequency, $V_A$ the Alfvén phase velocity, and $k_{\parallel m} = (n - m/q)/R$. The operator $L_{m\pm1}$ comes from toroidicity with $\hat{\epsilon} = 2(r/R + \Delta')$, and $\Delta$ being the Shafranov shift. Finally the fourth order term comes from finite ion gyroradius effects, and the parallel electric field due to kinetic electron response where $\rho$ is the mass density, $\rho_i$ is the ion gyroradius, $\rho_s$ is the sound gyroradius, and $Z(\xi)$ is the plasma dispersion function defined as

$$Z(\xi) = \frac{1}{\sqrt{\pi}} \int_{-\infty}^{\infty} dy \frac{e^{-y^2}}{y - \xi} \tag{3}$$

with $\xi = (\omega + i\nu)/(k_\parallel v_e)$, $\hat{\nu} = \nu/(k_\parallel v_e)$, and $\nu$ the electron collisional frequency.

The coupled equations can be derived from quasi-neutrality equation by neglecting the compressional Alfvén waves. The second order terms, which are of MHD origin, have been derived by others. The derivation of the fourth order term is given in the Appendix.

The coupled equations describe shear Alfvén waves in the low-beta large aspect ratio, circular tokamak limit. The fourth order term describes the kinetic effects of finite ion Larmor radius and the perturbed parallel electric field response that arises from the kinetic parallel electron dynamics which includes such effects as Landau damping, and collisions. The equations reduce to previous reduced MHD equations without the kinetic term. The model also reproduces the standard dispersion relation for kinetic Alfvén waves.

There are four boundary conditions for each poloidal component $\Phi_m$. Two of them come from the regularization condition at the origin $r = 0$. They can be expressed as $\Phi_m(0) = 0$ and $\Phi'_m(0) = 0$ for $m \neq 1$; and by $\Phi_m(0) = 0$ and $\Phi''_m(0) = 0$ for $m = 1$ with the superscript $'$ denotes radial derivative. To obtain the other two we take an ideal conducting wall at the plasma edge so that at this boundary: $\Phi_m = 0$ and $E_\parallel = 0$. From Eq. A8 in the Appendix, it is shown that the latter condition reduces to $\nabla \cdot \rho \nabla \Phi_m = 0$.

## III. Numerical Method

We have built a new code CubicKAE to solve Eq. (1) by using a cubic finite element method. Using this finite element, $\Phi_m$ can be written as:

$$\Phi_m(x) = \sum_i A_m(i) h(x,i) \tag{4}$$

where $x = r/a$ is the normalized radial variable, $h(x,i)$ is a cubic finite element defined on a uniform radial grid $x_i = i/N$ with $N$ being the total number of radial intervals and $i$ the radial grid index $i$ varying from $-1$ to $N+1$. Specifically, $h(x,i)$ can be written as

$$h(x,i) = (\frac{x - x_{i-2}}{\Delta})^3 \quad for \quad x_{i-2} < x < x_{i-1} \tag{5}$$

$$h(x,i) = 4 - 6(\frac{x - x_i}{\Delta})^2 + 3|\frac{x - x_i}{\Delta}|^3 \quad for \quad x_{i-1} < x < x_{i+1} \tag{6}$$

$$h(x,i) = -(\frac{x - x_{i+2}}{\Delta})^3 \quad for \quad x_{i+1} < x < x_{i+1} \tag{7}$$

$$h(x,i) = 0 \quad for \quad x < x_{i-2} \; or \; x > x_{i+2} \tag{8}$$

where $\Delta = 1/N$ is the distance between neighboring grid points. Figure 1 shows a typical finite element and its radial derivatives. Note that it is continuous up to the second derivative.

Using Eq. (3), the coupled equations (1) can be transformed into a matrix equation as

$$BX = \lambda CX \tag{9}$$

where B and C are two $M$ by $M$ matrices with $M = K(N-1)$, $K$ is the number of poloidal modes, $X$ is the eigenvalue vector, and $\lambda = \omega^2$ is the eigenvalue. Equation (9) can be obtained by multiplying Eq. (1) by $h(x,i)$ for each $i$ and integrating over the whole radial domain. Finally it should be noted that our coupled equation cannot be exactly cast into a linear eigenvalue matrix equation because of complex dependence of the plasma dispersion function on the eigenvalue $\lambda = \omega^2$. However, all other dependences on $\lambda$ are linear as written in Eq. (1). Thus, Eq. (1) can be cast into the matrix form of Eq. (9) where the Matrix $B$ depends on $\lambda$. Fortunately this dependence of $B$ on $\lambda$ is rather weak and Eq. (9) can be solved iteratively.

The code CubicKAE has been benchmarked for a uniform cylindrical plasma where an analytic solution of Eq. (1) can be obtained. We will also show below that the numerical results of kinetic damping also agree well with the analytic results of TAE's radiative damping.

## III. KINETIC DAMPING OF TAE

Here we apply CubicKAE code to study kinetic damping of TAE modes in a tokamak plasma. We will first consider a model tokamak equilibrium for which the analytic results are available as a benchmark for our code. Secondly, we will apply our code to a JET discharge where TAE damping rates were measured.

For the low beta, large aspect ratio ($R/a = 12.5$) and circular flux surface tokamak case, we take the q profile as parabolic with $q(0) = 1.05$ and $q(a) = 1.6$, the profile of density and temperature profile as uniform. We consider an even n=2 TAE mode located near the q=1.25 surface. When we compare the numerical results of this mode with analytic results, we simplify the kinetic coefficient $g_{Km}$ in Eq(1) to be

$$g_{Km} = \rho_i^2(1 - i\bar{\nu})\omega_{TAE}^2/v_A^2 \tag{10}$$

where $\omega_{TAE} = V_A/(2q_{gap}R)$(with $q_{gap} = 1.25$) is the nominal TAE mode frequency, and $\bar{\nu}$ is a small normalized dissipation parameter due to electron Landau damping and collision. In this model calculation, we set $\bar{\nu} = 0.1$. Figure (2) shows the MHD (i.e., $\rho_i = 0$) eigenfunction for the radial electric field $E_r = -d\Phi/dx$ with the eigenvalue $\lambda = 0.1475$ (which corresponds to $\omega/\omega_{TAE} = 0.96$). Figure (3) shows the corresponding kinetic eigenfunction at $\rho_i/a = 0.002$. It is evident that TAE is coupled to kinetic Alfvén waves and the short wavelength oscillation decays away from the gap location. This feature is consistent with the theory of radiative damping of the TAE. Figure (4) plots the normalized kinetic damping rate $\gamma/\omega$ as function of the gyroradius $\rho_i$ for both numerical results(solid line) and from an analytic WKB analysis (dashed line). We observe that numerical values agree quite well with the analytic results for radiative damping. This agreement further validates our code.

We now apply our model to the experimental JET plasma where damping rates of an $n = 1$ were measured. For a specific calculation we choose parameters and profiles of JET discharge (#38573) at t = 5sec, where: $B = 2.56T$, $n_e(0) \sim n_i(0) = 1.75e13cm^{-3}$, $T_e(0) = 2.3kev$, $T_i(0) = 2.3kev$, $q(0) = 1.36$, and $q(a) = 4.6$. The plasma density, temperature and

safety factor profiles are shown in Fig. 5 and 6. Figure 7 shows the corresponding $n = 1$ continuum spectrum. We note that the continuum gap is open through the entire plasma. This can arise because the plasma edge density is taken to be finite ($n_e(a)/n_e(0) \sim 0.07$ in Fig. (5)). As a result, when the fourth order kinetic term is set to zero, a discrete MHD TAE is found with a real eigenvalue $\lambda = 0.118$. Figure 8 shows the eigenfunction of this MHD mode. Figure 9 plots the corresponding kinetic eigenfunction for $\rho_i/a = \rho_s/a = 0.006$. We observe that overall structure of the kinetic eigenfunction is similar to the MHD one, but the kinetic eigenfunction has extra short wavelength oscillations near the q=1.5 gap location due to coupling to kinetic Alfvén waves. The calculated kinetic damping is shown in Fig. 10 as a function of the normalized gyroradius $\rho_i/a$ (We set $\rho_s = \rho_i$ in this parameter scan). At the experimental value of $\rho_i = 0.003$, the damping rate is about 0.1% which is much smaller than the measured damping rate of 1.0%. We remark here that both the calculated damping rates and kinetic mode structures are consistent with local analytic model of radiative damping. The damping is small due to small kinetic parameters of $\rho_i$ and $\rho_s$.

Since the kinetic damping can be sensitive to variation of plasma profiles, we have conducted a sensitivity study of the damping rate over a wide range of plasma parameters and profiles. An example of such a study is given in Fig. 11 which plots damping rate as function of $q(0)$. We see that within the range of $1.25 < q(0) < 1.45$, the damping rate remains very small ($\gamma_d/\omega \sim 0.1\%$. It should be pointed out that in all cases studied, the short wave length oscillations always appear near the main gap location (at $q = 1.5$). There is no apparent mode conversion to kinetic Alfvén waves near the center of plasma away from the main gap location as found in Ref. 11. Furthermore, there is no apparent mode conversion to KAW near the edge.

We now consider the sensitivity of the damping rate to the edge density. Specifically we have modified the density profile so that the plasma density can be zero at the edge. Figure 12 plots the modified density profile (dashed line) as well as the original density profile (solid line). Note that the new density profile goes smoothly to zero near the edge. We note that a zero edge density has a physical basis because the plasma density will fall to zero beyond the

last closed flux surface. This use of a zero edge density is a rough but simple way to model the scrape of layer region of the plasma. As a result of zero edge density, the continuum gaps cannot remain open throughout the entire plasma as can be observed in Fig. 13 and thus continuum resonances arise near the edge. Figure 14 shows the corresponding kinetic eigenfunction (at $q(0) = 1.35$). Indeed the eigenfunction exhibits sharp oscillations near the continuum resonance especially for the m=4 component. The calculated eigenvalue is $\lambda = 0.119 - 0.0012i$ which corresponds to a damping rate of $\gamma_d/\omega = 0.5\%$. We note that this damping rate is significantly higher than found in the previous calculation and is about half the measured damping rate of 1.0%.

In addition to the sensitivity of the damping to the edge density profile, other edge effects should be important. These include,, the edge q-variation and open field line effects of the scrape-off plasma. These "small" edge effects will be a challenge to calculate in a quantitatively accurate manner and we will need a more realistic code than we are presently using to achieve precision in the damping rate prediction. For now, we have limited ourselves to the observation that the sensitivity of damping to the edge density can lead to damping rates comparable to what is observed experimentally.

A word on numerical resolution is in order here. In above calculations, we typically use five poloidal modes ($m = 1 \sim 5$) and 600 radial grid points. We find that the calculated damping rate is well converged at this resolution. Up to 9 poloidal modes and 1000 radial grid points were used in our convergence study.

## IV. COMPARISON WITH OTHER WORK

To summarize our results, our global kinetic model recovers the analytic "radiative" damping results of TAE for a model large aspect ratio tokamak equilibrium. We have calculated damping rates of an n=1 TAE for an experimental JET plasma with two density profiles: one with finite edge density and one with zero edge density. For the former case, the continuum gaps are open throughout the entire plasma and the calculated damping

rates are much smaller than the measured value. For the latter case with zero edge density, the calculated damping rate increases substantially due to continuum resonances that then appears near the plasma edge.

A. Jaun et al. [11] has previously calculated, using waves driven by an external antenna, the kinetic damping for the JET discharge with the same parameters and profiles, including a finite edge density, as studied in this work. The calculated kinetic damping rates in their work are substantially larger than what has been reported here. In Ref. [11], it is claimed that the dominant damping mechanism arises from mode conversion to kinetic Alfvén waves that occurs near the center of plasma. This claim is supported with numerical which exhibit short wavelength oscillations near the center of the plasma (see Fig. 4 of Ref. 11). In contrast, we did not find any such nonlocal mode conversion away from the main continuum gap (i.e., at q=1.5) in all cases studied. We only find mode conversion to KAW arises near the main gap location where the mode peaks and has its shortest MHD spatial structure and this conversion is consistent with the predictions of analytic theory. As a result, when we use a finite edge density, the damping rate we find is much smaller than that found in Ref.( [11] ). We can only conjecture about what causes the discrepancy between the two results. Both our models appear to address the same key physics issues. Jaun et al. used a gyrokinetic-MHD model based on expansion of ion gyroradius up to second order. The model includes both shear Alfvén waves and compressional Alfvén waves and is valid for finite aspect ratio numerical equilibria. Our model includes the similar kinetic physics, although only shear Alfvén waves are included and toroidicity is retained only up to first order of $r/R$. We believe that these differences between our models should not lead to significant differences in the mode conversion process associated with the plasma core.

One possibility for the discrepancy is that the mode found by Jaun et al. is mainly a kinetic Alfvén mode rather than a kinetically modified TAE found by us. He uses an antenna code to excite oscillations and it is conceivably that the excitations he finds are not dominated by a single TAE mode as is commonly assumed. It should be noted that we have also found many other kinetic eigenmodes besides the least damped kinetic TAE

mode. These kinetic modes have mode structures dominated by short wavelength kinetic Alfvén waves and consequentially their damping rates are much larger.

In addition there is a technical difference in the treatment of boundary conditions at the magnetic axis that can conceivable cause for the discrepancy of our result with that found in Ref. [11]. In our technique we use a modal expansion in poloidal angle, which produces singular operator for each harmonic at the magnetic axis which enforces the choice of regularity for the boundary condition. In Juan's work a finite element method is used to represent the plasma wave operator without any poloidal angle decomposition. It is unclear whether the resolution used in Jauns work is adequate for resolving the poloidal and radial mode structure near the center.

The TAE damping in JET plasmas has also been considered by Borba et al. [12] where the CASTOR [13] code was used to evaluate the damping rates as determined from the response to an antenna situated in the vacuum. CASTOR is a full geometry MHD code that has been generalized to include "complex resistivity " that describes conventional resistivity plus the kinetic effects from the parallel electron dynamics and and finite ion gyro-radius. As in our work, no obvious mode conversion was observed near the magnetic axis. Nonetheless, they found for a JET ohmic discharge(slightly different from our case), that the calculated damping rates were $\gamma_d/\omega \sim 1.0\%$ which is comparable to the experimental measurement. Such a large damping rate was at first somewhat surprising to us because the continuum gaps are wide open throughout the entire plasma and in the published eigenmode structure (See Fig. 8 of Ref. 13) there are no obvious short wavelength oscillations indicating mode conversion to kinetic Alfvén waves. However, upon close examination of the mode structure near the edge, short wavelength oscillations can be found (they were clearer when the derivative of the eigenfunction was shown to us) and it was claimed that the oscillations lead to mode conversion to KAW near the edge of the plasma which is the main contribution to the damping rate that was reported. Thus, our results correlate with Borba et al. in that both of our studies do not produce significant KAE mode conversion near the center of plasma. However, as we have found insignificant mode conversion arising from the edge

of the plasma when the TAE gaps were open, we need to determine what is the essential difference of our results of our model from the work of Borba, et. al. who find that the dominant damping mechanisms come from this region. In Borba's work there was a need to couple the response inside the plasma to the vacuum response where the antenna was located. To do this the boundary condition for an resistive MHD plasma was used between the plasma and vacuum interface. It is conceivable that this boundary condition together with compressional Alfvén wave coupling, that is in both Jaun's and Borba's codes, causes mode conversion to Kinetic Alfvén waves near the edge. Furthermore, Borba's work includes full toroidal effects which are not included in our study, and perhaps this difference is a cause for significant discrepancy. To obtain a consistent edge boundary condition we have taken the plasma to be in contact with a physical conducting wall at the edge where the density can be finite. Surprisingly, only insignificant, if any, mode conversion arises with such a boundary condition and this is apparently due to the imposition of the zero parallel electric field at the wall We have shown in calculations not included here that for some other type of boundary conditions, both analytically and numerically, that mode conversion can occur near the edge and this results in larger damping rates

## V. CONCLUSIONS

In conclusion, we find that in our model set of equations there is negligible mode conversion from TAE to KAW near the center of plasma for the parameters and profiles of a JET plasma. When a small but finite plasma edge density is taken the calculated kinetic damping rates are much smaller than the measured values when there are no continuum resonances. However, when the edge density is taken small enough, our model set of equations produce a damping of about half of the experimental damping rate due to the continuum damping that arises. We believe that in the JET experiment the main damping mechanisms are likely to arise from the wave interactions with the plasma in the edge region.

Our results show significantly less mode conversion near the magnetic axis or near the

edge than other studies [11,12]. Clearly more work is needed to better understand the root cause of these discrepancies and how to describe the wave properties at the plasma edge in a more realistic manner.

The authors gratefully acknowledge useful discussions with D. Borba, A. Jaun and S. Sharapov. This work is supported by the U.S. Department of Energy under Contract No. DE-AC02-76-CHO-3073.

## APPENDIX A: DERIVATION OF KINETIC MODEL

Our aim is to obtain the higher order derivative terms (KAE terms) that need to be added to the reduced MHD equations in the limit of a small inverse aspect ratio tokamak when the plasma beta is insignificant. We will write the response in the shear slab limit and then replace the MHD terms by the standard forms that include the geometrical effects (e.g., see Ref. 6). The ion FLR correction to the KAE term is well known [14] and our principal goal is to obtain the form appropriate to the treatment of electrons, where the physics needs to include collisions and electron Landau damping as well as the electron response when they have thermal velocities greater or less than the wave phase velocity along the magnetic field (the former limit is generally appropriate in most of the core of the plasma while the latter limit can become appropriate near the edge and in small regions where $k_\parallel$ is small). We also assume that $\omega_\star << \omega$ so that the diamagnetic drift terms of ions and electrons can be neglected. In addition we neglect the magnetic compressional term, which is insignificant for the waves considered here when the plasma is of negligible beta and when the wave-number vector is nearly perpendicular to the magnetic field.

Let us take the perturbed electric field of the form $\mathbf{E} = E_\parallel \mathbf{b} - \nabla_\perp \phi$, where $\nabla_\perp = \nabla - \mathbf{bb}\cdot\nabla$. The field amplitudes, $E_\parallel$ and $\phi$ are taken to satisfy Poisson's equation and the parallel current equations. The parallel current, $j_\parallel$, is assumed to be dominated by the electron current, $j_{\parallel e}$. In terms of the perturbed distribution, $f$, the two equations are given by

$$\sum_j e_j \int d^3v f_j = -\nabla_\perp^2 \phi + i k_\parallel E_\parallel \tag{A1}$$

$$\nabla_\perp^2 (E_\parallel + \mathbf{b}\cdot\nabla\phi) = -\frac{4\pi i\omega}{c^2} j_\parallel \tag{A2}$$

and $f_e$ is taken to satisfy the Vlasov equation with collisions

$$-i(\omega - k_\parallel v) f - e\frac{E_\parallel v_\parallel}{T_e} f_M = -\nu(f - \frac{\delta n_e}{n_e} f_M) \tag{A3}$$

where $e$ is the electron charge, $f_M$ is an equilibrium Maxwellian distribution,

$$f_e = \frac{n_e}{(\pi v_e^2)^{3/2}} \exp(-\frac{v^2}{v_e^2}) \tag{A4}$$

where $T_e = m_e v_e^2/2$ and $\nu$ is the electron collision frequency, and $\delta n_e$ is the perturbed electron density. For simplicity we have neglected cross field derivatives in the Vlasov equation because cross field drifts from electrons and ions cancel to the leading order.

To solve for $j_{\parallel e}$, we use that Eq. (A3) leads to the continuity relation, $j_{\parallel e} = e\omega\delta n_e/k_\parallel$, so that we can solve Eq. (A3) for $\delta n_e = \int d^3v f_e$ and then construct $j_{\parallel e}$. After some algebra we find,

$$4\pi j_{\parallel e} = -\frac{2i\omega_{pe}^2\omega}{k_\parallel^2 v_e^2} \frac{1 + \xi Z(\xi)}{1 + i\hat{\nu} Z(\xi)} E_\parallel \tag{A5}$$

where

$$Z(\xi) = \frac{1}{\sqrt{\pi}} \int_{-\infty}^{\infty} dy \frac{e^{-y^2}}{y - \xi} \tag{A6}$$

with $\xi = \omega/(k_\parallel v_e) + i\hat{\nu}$ and $\hat{\nu} = \nu/(k_\parallel v_e)$. Substituting Eq. (A5) into Eq. (A2) yields the relation,

$$\left[ c^2\nabla_\perp^2 + 2\omega_{pe}^2 (\frac{\omega}{k_\parallel v_e})^2 \frac{1 + \xi Z(\xi)}{1 + i\hat{\nu} Z(\xi)} \right] E_\parallel = -ic^2 \nabla_\perp^2 (k_\parallel \phi) \tag{A7}$$

We will discard the first term in the bracket on the left hand side of the equation as we assume that $E_\parallel << -ik_\parallel\phi$, in accord with the usual MHD conditions.

The evaluation of the charge density in the Poisson equation is standard and it yields,

$$4\pi \sum_j e_j f_j = \nabla_\perp \cdot \frac{\omega_{pi}^2}{\omega_{ci}^2} \cdot \nabla\phi - i\frac{2\omega_{pi}^2}{k_\parallel v_e^2}\frac{1+\xi Z(\xi)}{1+i\hat{\nu}Z(\xi)}E_\parallel = -\nabla_\perp^2\phi + ik_\parallel E_\parallel \tag{A8}$$

Discarding the last term on the right hand side, we then find by eliminating $E_\parallel$ in the substitution of Eq.(A7) into (A8),

$$k_\parallel \nabla_\perp^2 \frac{k_\parallel v_e^2}{2\omega_{pe}^2}\frac{1+i\hat{\nu}Z(\xi)}{1+\xi Z(\xi)}\nabla \cdot \frac{\omega_{pi}^2}{\omega_{ci}^2}\nabla\phi + \nabla_\perp \cdot \frac{\omega^2}{v_A^2}\nabla_\perp\phi - k_\parallel \nabla_\perp^2(k_\parallel\phi) = 0 \tag{A9}$$

If we now match this form of the equation to one where the MHD equations are derived with a serious consideration to geometry we arrive at the equations presented in the text.

We note that Eq. (A9) together with finite ion Larmor radius effects gives the following local dispersion relation for kinetic Alfvén waves:

$$\omega^2 = k_\parallel^2 v_A^2(1 + \frac{3}{8}k_\perp^2\rho_i^2 + \frac{1}{2}k_\perp^2\rho_s^2\frac{1+i\hat{\nu}Z(\xi)}{1+\xi Z(\xi)}) \tag{A10}$$

In the limit of zero collision and $\xi << 1$, Eq. (A10) reduces to the well known dispersion relation for kinetic Alfvén waves:

$$\omega^2 = k_\parallel^2 v_A^2(1 + \frac{3}{8}k_\perp^2\rho_i^2 + \frac{1}{2}k_\perp^2\rho_s^2) \tag{A11}$$

Furthermore, in the limit of strong collision, $\nu >> \omega$ and $\nu >> k_\parallel v_e$, Eq. (A9) reduces to resistive MHD model.

Finally, it should be pointed out our kinetic model gives a finite perpendicular wavelength at $k_\parallel = 0$ instead of infinity wavelength from the standard kinetic Alfvén wave dispersion relation (Eq. A11).

# REFERENCES


[1] C. Z. Cheng, L. Chen, and M. S. Chance, Ann. Phys. (N. Y.) **161**, 21 (1985).

[2] G. Y. Fu and J. W. Van Dam, Phys. Fluids B**1**, 1949 (1989).

[3] C. Z. Cheng, Phys. Fluids, B**3**, 2463 (1991); R. Betti and J. P. Freidberg, Phys. Fluids B**3**, 1865 (1991).

[4] N. N. Gorelenkov and S. E. Sharapov, Physica Scripta, 45 (1991).

[5] G. Y. Fu and C. Z. Cheng, Phys. Fluids B**4**, 3722 (1992).

[6] H. L. Berk, J. W. Van Dam, Z. Guo, and D. M. Lindberg, Phys. Fluids B**4**, 1806 (1992).

[7] R. Mett and S. Mahajan, Phys. Fluids B **4**, 2885 (1992).

[8] H. L. Berk, R. R. Mett, and D. M. Lindberg, Phys. Fluids B **5**, 3969 (1993).

[9] D. Testa, G. Y. Fu, A. Jaun et al., Nucl. Fusion **43**, 594 (2003).

[10] G. Y. Fu, C. Z. Cheng, R. Budny et al., Phys. of Plasmas **3**, 4036 (1996).

[11] A. Jaun, A. Fasoli and W. W. Heidbrink, Phys. of Plasmas **5**, 2952 (1998).

[12] D. Borba, H. L. Berk, B. N. Breizman et al., Nucl. Fusion **42**, 1029 (2002).

[13] W. Kerner et al., J. Comput. Phys. **142**, 271 (1998).

[14] L. Chen and A. Hasagawa, Phys. Rev. Lett. **32**, 454 (1974).

## FIGURES

FIG. 1. *A typical cubic finite element $h(x,i)$ and its first and second derivative as function of $x$.*

FIG. 2. *Radial electric field of an $n = 2$ MHD TAE as function of radius for poloidal component $m = 2$(solid line) and $m = 3$(dashed line).*

FIG. 3. *Radial electric field of an $n = 2$ kinetic TAE as function of radius for poloidal component $m = 2$(solid line) and $m = 3$(dashed line).*

FIG. 4. *Kinetic Damping of the n=2 TAE as function of normalized gyroradius $\rho_i/a$ obtained from numerical calculations(solid line) and an analytic radiative damping model(dashed line).*

FIG. 5. *the normalized plasma mass density ($\rho(x)/\rho(0)$, solid line) and temperature ($T(x)/T(0)$, dashed line) profiles of a JET discharge(#38573) at $t = 5sec$.*

FIG. 6. *Safety factor profile $q(x)$ of a JET discharge(#38573) at $t = 5sec$.*

FIG. 7. *The n=1 shear Alfvén continuum frequency $\lambda = \omega^2/\omega_A^2$ as function of plasma radius ($\omega_A = v_A(0)/R_0$) correponding to plasma profiles given in Fig. 5 and 6.*

FIG. 8. *Radial electric field of an $n = 1$ MHD TAE as function of radius for poloidal component $m = 1$(solid line), $m = 2$(dashed line), $m = 3$(dashed-dot line), $m = 4$(solid line), and $m = 5$ (dashed line) obtained with profiles given in Fig. 5 and 6. The lines are also marked with poloidal mode numbers.*

FIG. 9. *Radial electric field of an $n = 1$ kinetic TAE as function of radius for poloidal component $m = 1$(solid line), $m = 2$(dashed line), $m = 3$(dashed-dot line), $m = 4$(solid line), and $m = 5$ (dashed line) obtained with profiles given in Fig. 5 and 6. The lines are also marked with poloidal mode numbers.*

FIG. 10. *Kinetic Damping rate of the n=1 TAE as function of normalized gyroradius* $rho_i$ *for profiles in Fig. 5 and 6.*

FIG. 11. *Kinetic Damping rate of the n=1 TAE as function of* $q(0)$ *for profiles in Fig. 5 and 6.*

FIG. 12. *Comparison of density profiles with finite(solid line) and zero(dashed line) edge density.*

FIG. 13. *The n=1 shear Alfvén continuum frequency* $\lambda = \omega^2/\omega_A^2$ *as function of plasma radius correponding to zero edge density.*

FIG. 14. *Radial electric field of an* $n = 1$ *kinetic TAE as function of radius for poloidal component* $m = 1$*(solid line),* $m = 2$*(dashed line),* $m = 3$*(dashed-dot line),* $m = 4$*(solid line), and* $m = 5$ *(dashed line) for zero edge density. The lines are also marked with poloidal mode numbers.*

Fig.1, Fu, PoP

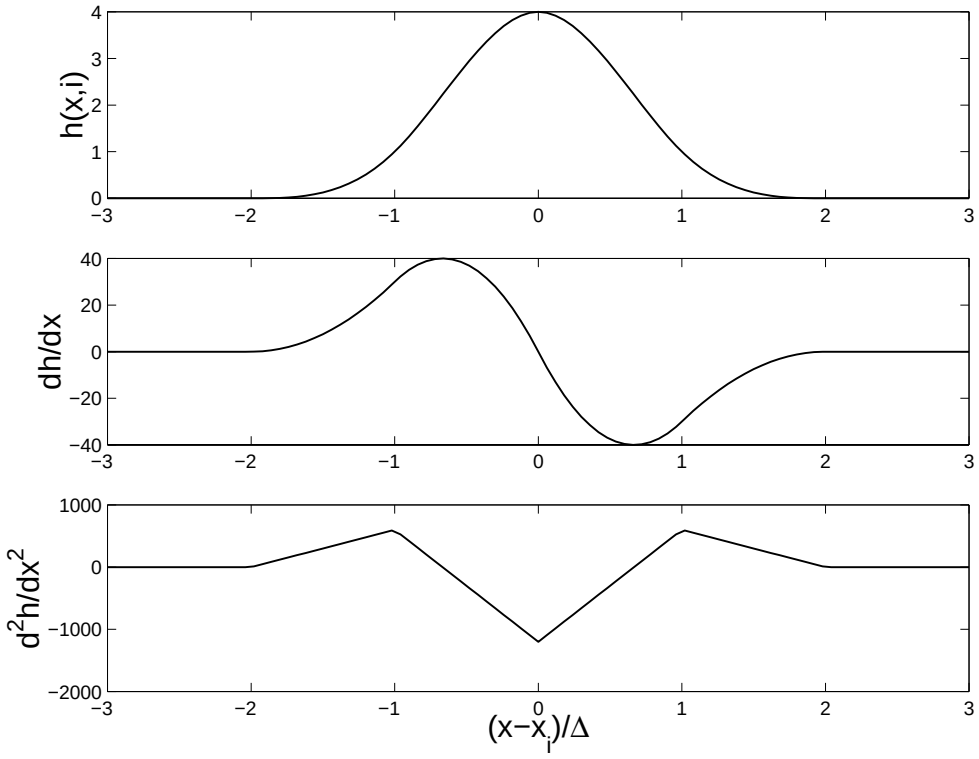

Fig.2, Fu, PoP

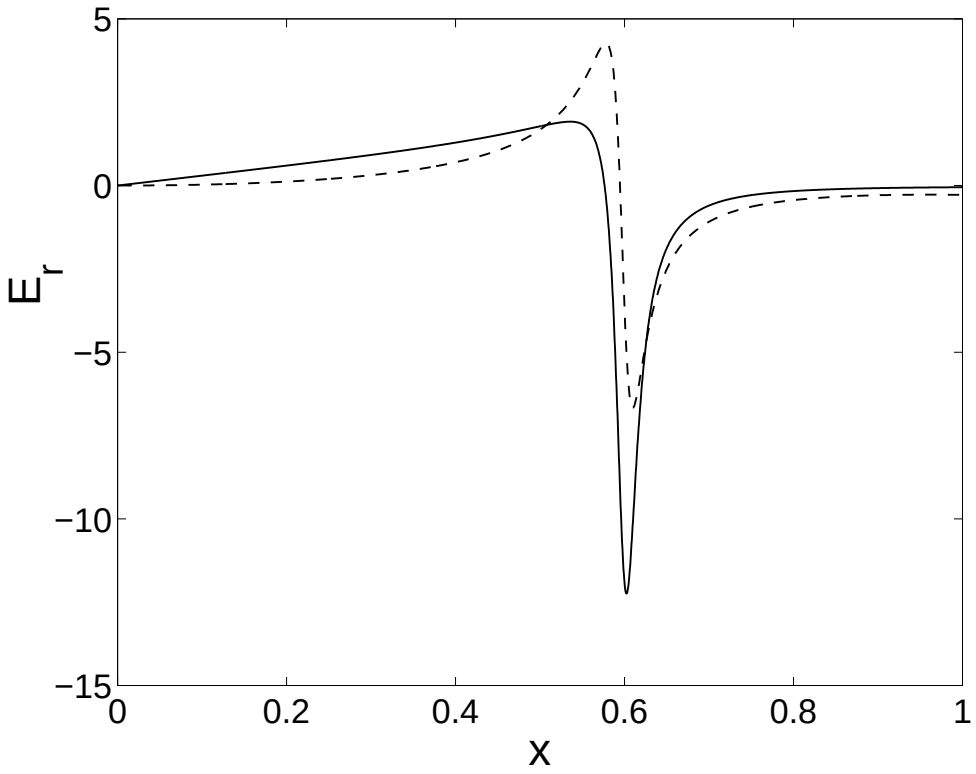

Fig.3, Fu, PoP

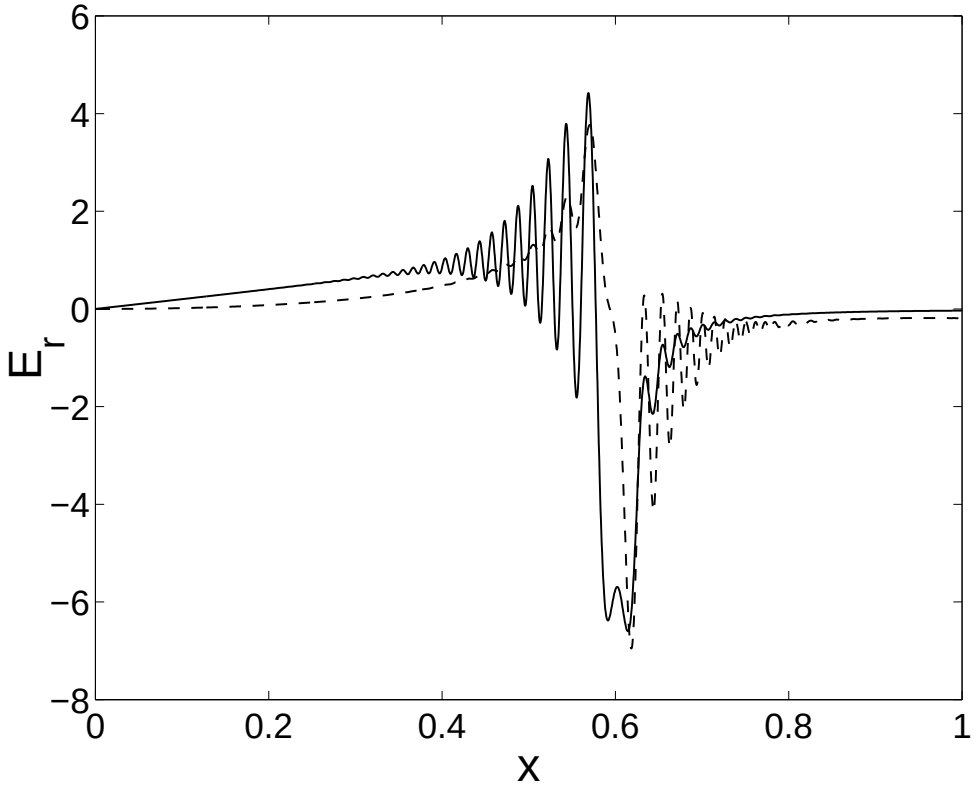

Fig.4, Fu,

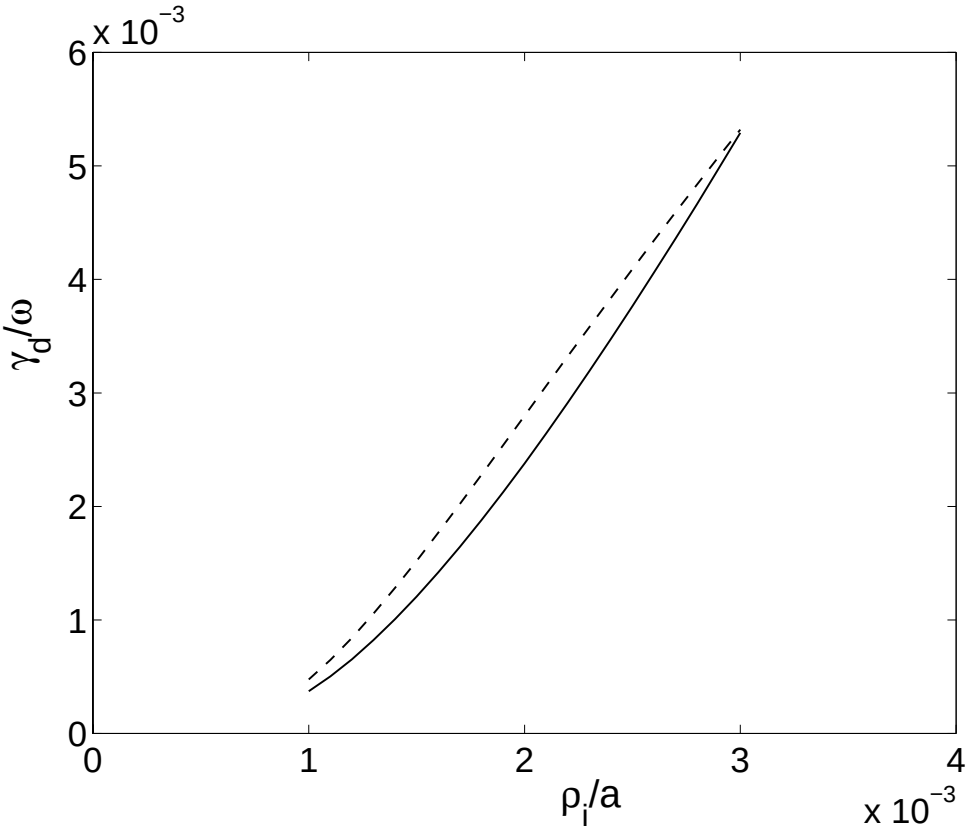

Fig.5, Fu, PoP

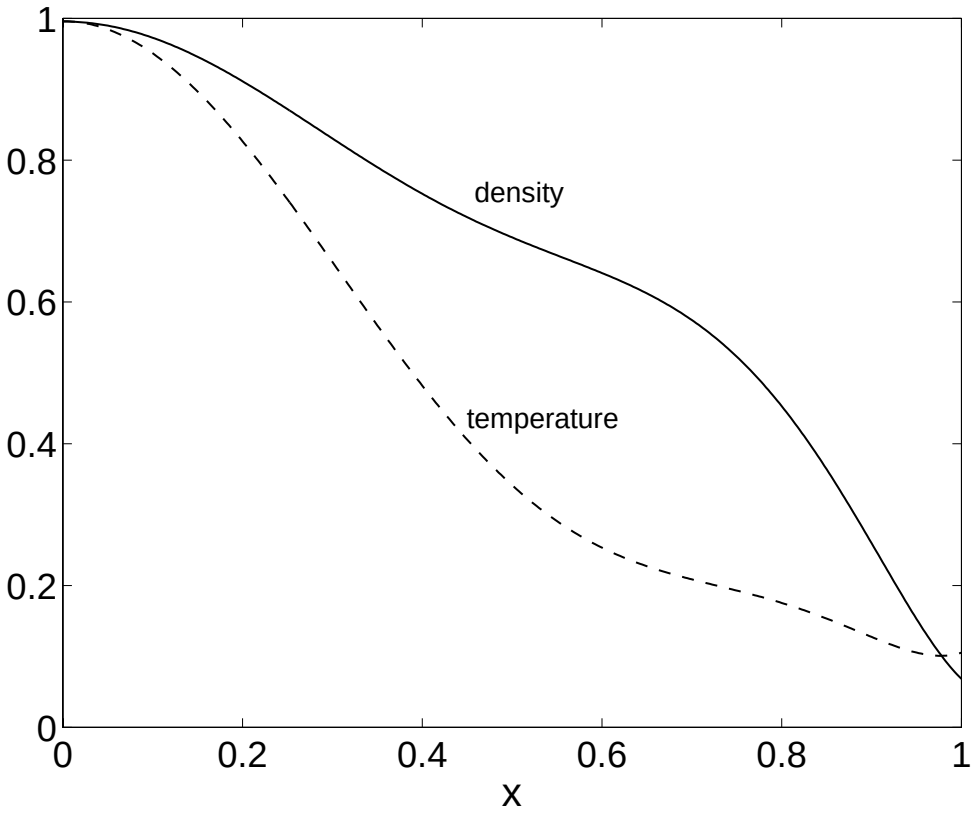

Fig.6, Fu, PoP

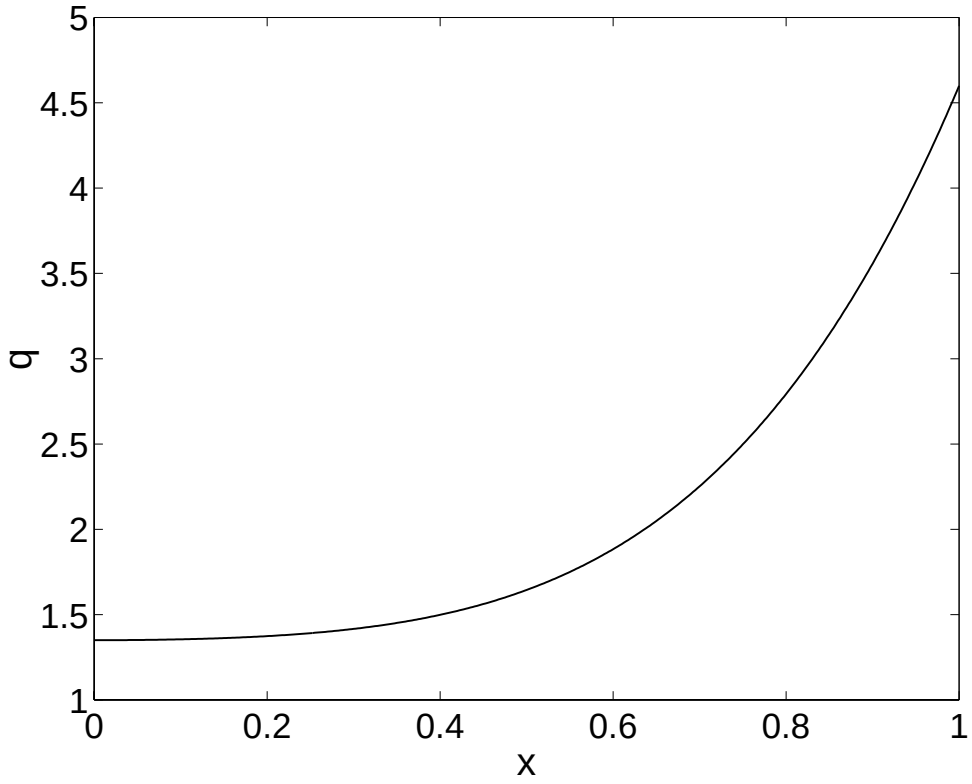

Fig.7, Fu, PoP

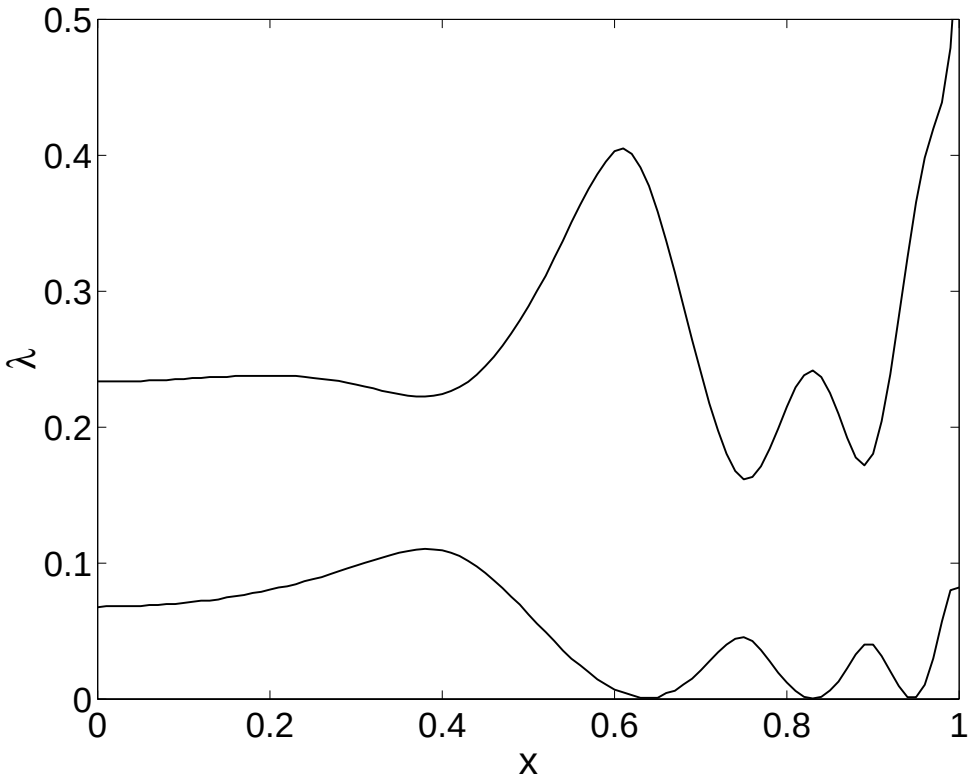

Fig.8, Fu, PoP

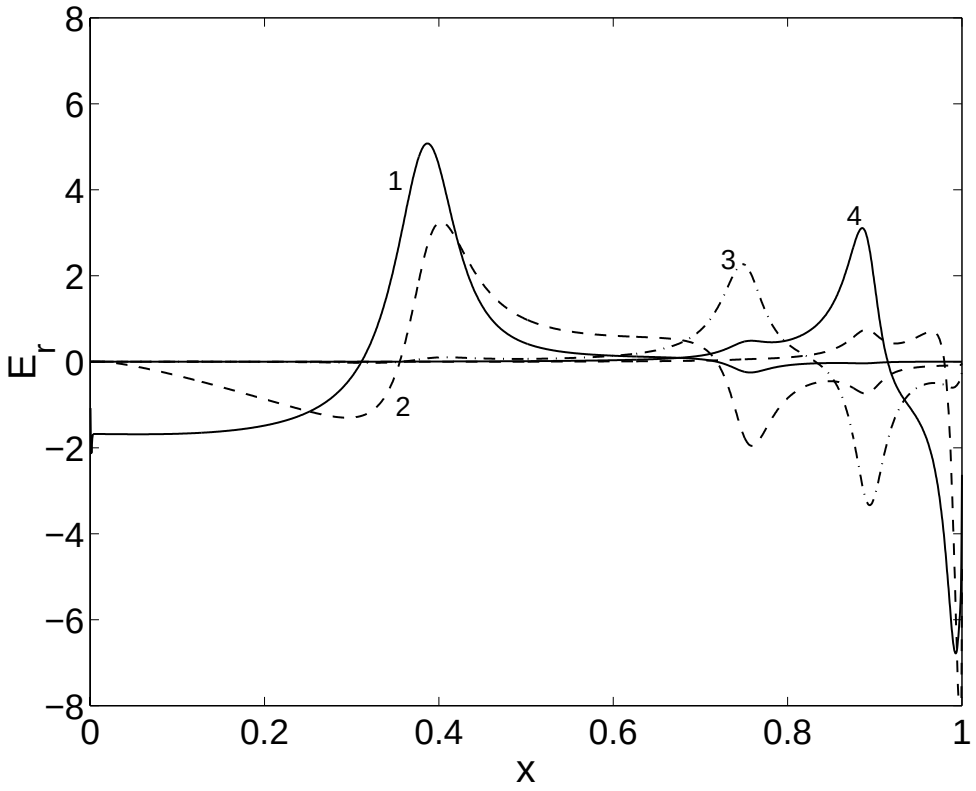

Fig.9, Fu, PoP

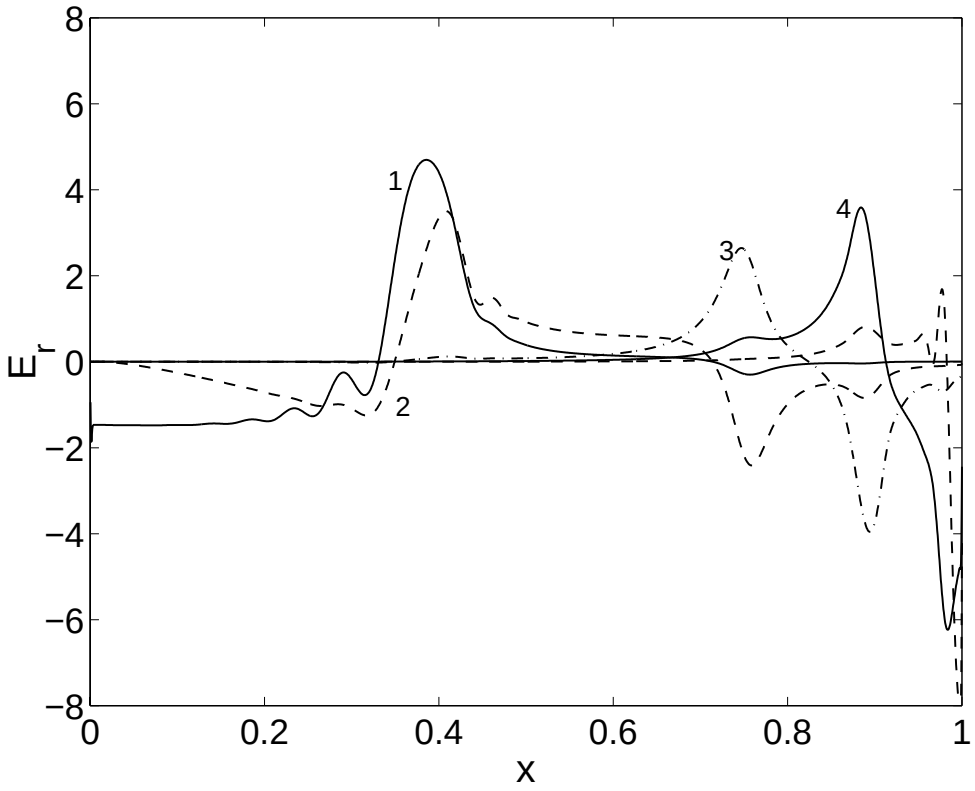

Fig.10, Fu, PoP

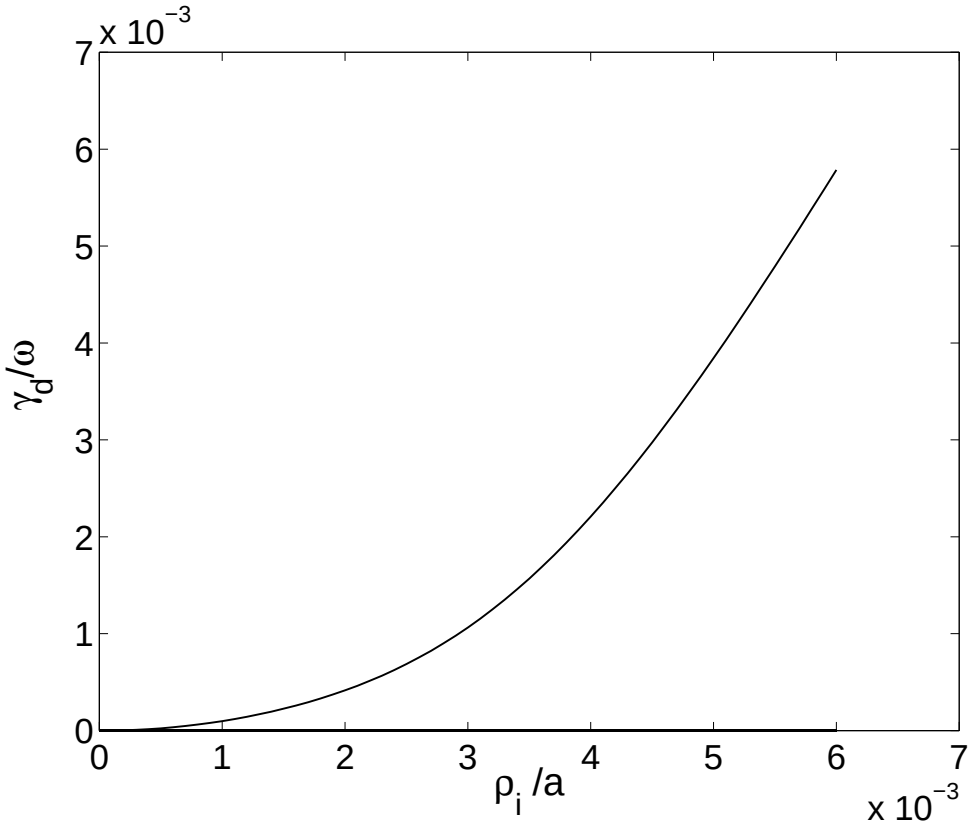

Fig.11, Fu, PoP

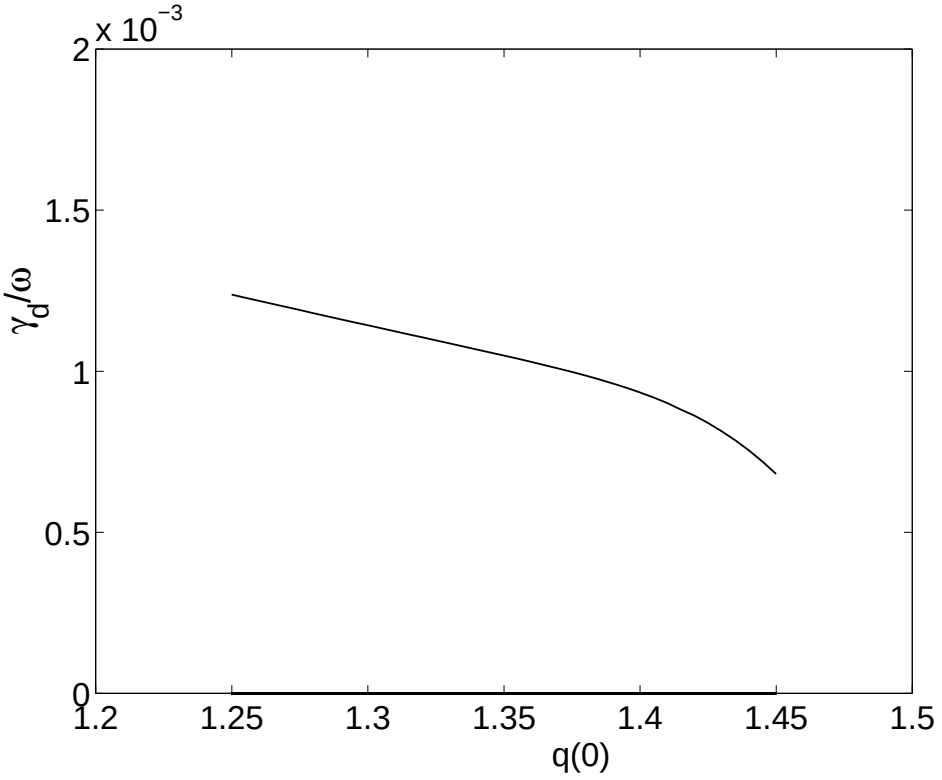

Fig.12, Fu, PoP

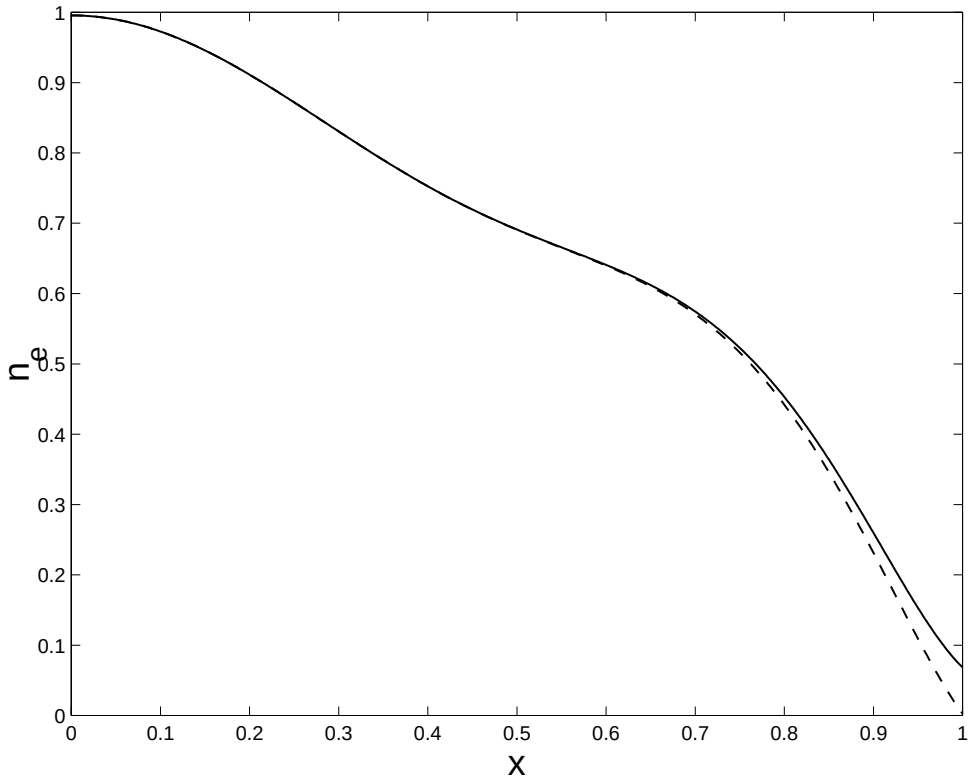

Fig.13, Fu, PoP

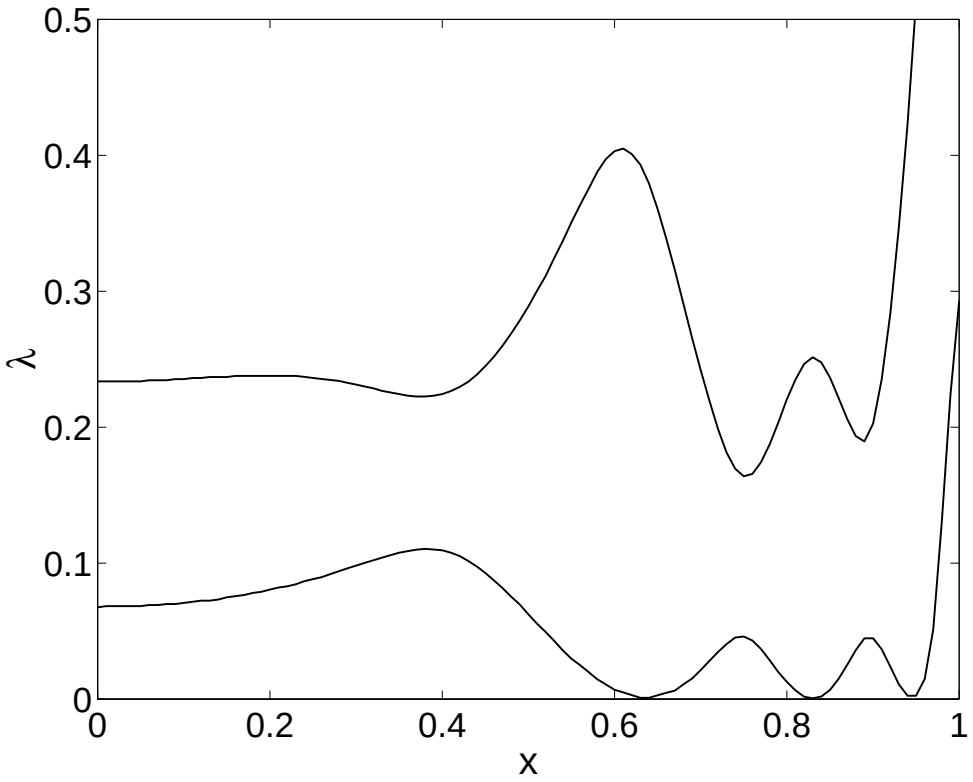

Fig.14, Fu, PoP

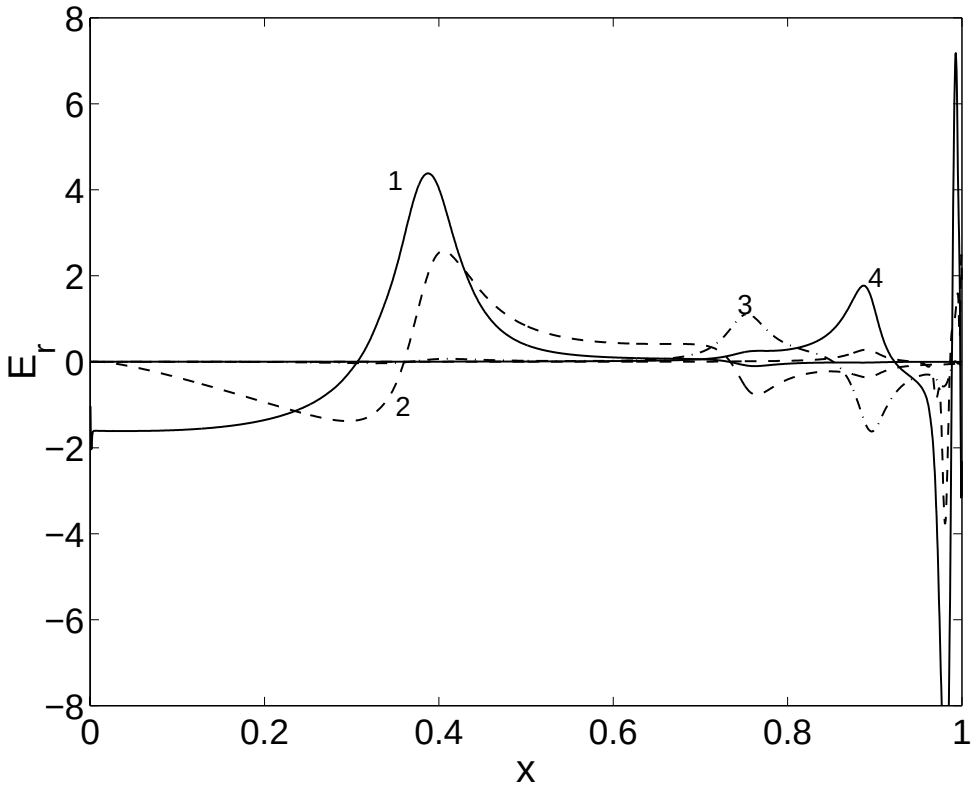

## External Distribution

Plasma Research Laboratory, Australian National University, Australia

Professor I.R. Jones, Flinders University, Australia

Professor João Canalle, Instituto de Fisica DEQ/IF - UERJ, Brazil

Mr. Gerson O. Ludwig, Instituto Nacional de Pesquisas, Brazil

Dr. P.H. Sakanaka, Instituto Fisica, Brazil

The Librarian, Culham Science Center, England

Mrs. S.A. Hutchinson, JET Library, England

Professor M.N. Bussac, Ecole Polytechnique, France

Librarian, Max-Planck-Institut für Plasmaphysik, Germany

Jolan Moldvai, Reports Library, Hungarian Academy of Sciences, Central Research Institute for Physics, Hungary

Dr. P. Kaw, Institute for Plasma Research, India

Ms. P.J. Pathak, Librarian, Institute for Plasma Research, India

Dr. Pandji Triadyaksa, Fakultas MIPA Universitas Diponegoro, Indonesia

Professor Sami Cuperman, Plasma Physics Group, Tel Aviv University, Israel

Ms. Clelia De Palo, Associazione EURATOM-ENEA, Italy

Dr. G. Grosso, Instituto di Fisica del Plasma, Italy

Librarian, Naka Fusion Research Establishment, JAERI, Japan

Library, Laboratory for Complex Energy Processes, Institute for Advanced Study, Kyoto University, Japan

Research Information Center, National Institute for Fusion Science, Japan

Dr. O. Mitarai, Kyushu Tokai University, Japan

Dr. Jiangang Li, Institute of Plasma Physics, Chinese Academy of Sciences, People's Republic of China

Professor Yuping Huo, School of Physical Science and Technology, People's Republic of China

Library, Academia Sinica, Institute of Plasma Physics, People's Republic of China

Librarian, Institute of Physics, Chinese Academy of Sciences, People's Republic of China

Dr. S. Mirnov, TRINITI, Troitsk, Russian Federation, Russia

Dr. V.S. Strelkov, Kurchatov Institute, Russian Federation, Russia

Professor Peter Lukac, Katedra Fyziky Plazmy MFF UK, Mlynska dolina F-2, Komenskeho Univerzita, SK-842 15 Bratislava, Slovakia

Dr. G.S. Lee, Korea Basic Science Institute, South Korea

Dr. Rasulkhozha S. Sharafiddinov, Theoretical Physics Division, Insitute of Nuclear Physics, Uzbekistan

Institute for Plasma Research, University of Maryland, USA

Librarian, Fusion Energy Division, Oak Ridge National Laboratory, USA

Librarian, Institute of Fusion Studies, University of Texas, USA

Librarian, Magnetic Fusion Program, Lawrence Livermore National Laboratory, USA

Library, General Atomics, USA

Plasma Physics Group, Fusion Energy Research Program, University of California at San Diego, USA

Plasma Physics Library, Columbia University, USA

Alkesh Punjabi, Center for Fusion Research and Training, Hampton University, USA

Dr. W.M. Stacey, Fusion Research Center, Georgia Institute of Technology, USA

Dr. John Willis, U.S. Department of Energy, Office of Fusion Energy Sciences, USA

Mr. Paul H. Wright, Indianapolis, Indiana, USA

The Princeton Plasma Physics Laboratory is operated
by Princeton University under contract
with the U.S. Department of Energy.

Information Services
Princeton Plasma Physics Laboratory
P.O. Box 451
Princeton, NJ 08543

Phone: 609-243-2750
Fax: 609-243-2751
e-mail: pppl_info@pppl.gov
Internet Address: http://www.pppl.gov